Feature Analysis of Functional MRI Data for Mapping Epileptic Networks

A Dissertation Proposal
Presented to
The Academic Faculty

By

Lauren S. Burrell

In Partial Fulfillment
of the Requirements for the Degree
Doctor of Philosophy

School of Electrical and Computer Engineering
Georgia Institute of Technology

August 2006

TABLE OF CONTENTS

LIST OF FIGURES

LIST OF TABLES

LIST OF ACRONYMS

ASL: Arterial Spin Labeling

AUC: Area Under the Curve

BOLD: Blood Oxygen Level Dependent

CASL: Continuous Arterial Spin Labeling

CBF: Cerebral Blood Flow

EEG: Electroencephalogram

fMRI: Functional Magnetic Resonance Imaging

GA: Genetic Algorithm

GP: Genetic Programming

HRF: Hemodynamic Response Function

ICA: Independent Component Analysis

IEEG: Intracranial EEG

k-NN: k-Nearest Neighbor

mTL: Mesial Temporal Lobe

PCA: Principal Component Analysis

PET: Positron Emission Tomography

ROC: Receiver Operating Characteristic

ROI: Region of Interest

SPECT: Single Photon Emission Computed Tomography

SPM: Statistical Parametric Mapping

TCA: Temporal Clustering Analysis

TLE: Temporal Lobe Epilepsy

SUMMARY

Epilepsy, a chronic neurological disorder characterized by recurrent, unprovoked seizures, affects up to one percent of the world's population. Antiepileptic drug therapies are ineffective in over 30% of epilepsy patients. In these cases, the medications either do not successfully control seizures or have unacceptable side effects. Approximately one-third of patients whose seizures cannot be controlled by medication are candidates for surgical removal of the affected area of the brain, potentially rendering them seizure free. Accurate localization of the epileptogenic focus, i.e. the area of seizure onset, is critical for the best surgical outcome. Currently the most widely used tool for localization of the epileptogenic zone is electroencephalography. While the electroencephalogram (EEG) has high temporal resolution, it suffers from poor spatial resolution. Combining EEG recordings with a diagnostic tool possessing higher spatial resolution, such as functional magnetic resonance imaging (fMRI), might allow for more precise localization of the epileptogenic focus. The primary objective of the proposed research is to develop a set of fMRI data features that can be used to distinguish between normal brain tissue and the epileptic focus. To determine the optimal combination of features from various domains, genetic programming will be used. A classifier will then be employed to label brain voxels as either normal or epileptogenic based on this optimal feature. The accuracy of these classification results will be assessed by comparing the seizure focus as determined by this methodology with the focus determined by neurologists through analysis of EEG data from the same patients.

SECTION I

1 Introduction

1.1 Motivation

Epilepsy, a chronic neurological disorder characterized by recurrent, unprovoked seizures, affects approximately 1% of the world's population [1]. For 30 to 40% of epilepsy patients, antiepileptic drugs either cannot effectively control seizures or have intolerable side effects [2]. One-third of patients for whom drug therapy is ineffective are candidates for surgical treatment [3]; however, only 60 to 80% of patients are currently rendered seizure-free following surgery [4]. More accurate localization of the area of seizure onset is clearly needed to increase the efficacy of surgery. Uncontrolled epilepsy can lead to depression, anxiety, and loss of cognitive function and is associated with higher healthcare costs [2].

1.2 Problem Statement

Accurate focus localization is essential for rendering patients seizure-free following epilepsy surgery. Correct localization is also vital in directing the placement of electrodes for implantable devices designed to stop seizure propagation. Electroencephalogram (EEG) recording, the most widely used functional tool for epileptic focus localization, suffers from low spatial resolution. Functional magnetic resonance imaging (fMRI), on the other hand, has much higher spatial resolution and can potentially be used in conjunction with EEG for more precise localization.

The primary objective of the proposed research is to develop a voxel-based fMRI time series analysis technique for mapping epileptic networks. A set of quantitative features will be

formulated for distinguishing between normal brain tissue and epileptogenic regions. Features will be extracted from the time, frequency, statistical, and mutual information domains, and the most useful combination of features for focus localization will be determined through the application of genetic programming. The feasibility of selecting an optimal feature set will be tested by examining data from patients with temporal lobe epilepsy (TLE), a common epilepsy syndrome, which is often amenable to surgery.

The central hypothesis for the proposed research is that differences in the temporal dynamics of fMRI signals in epileptogenic and normal brain regions can be identified through feature analysis of the voxel time series and used to classify brain regions as normal or belonging to the epileptic network.

2 Origin and History of the Problem

2.1 Functional Magnetic Resonance Imaging

Functional magnetic resonance imaging (fMRI) is a noninvasive neuroimaging technique that measures hemodynamic changes resulting from changes in the level of neuronal activity. Through the analysis of fMRI data, which consist of sequences of images acquired over time, the spatiotemporal dynamics of brain activation can be explored. The contrast in these images is attributable to differences in tissue function rather than structure. High-resolution anatomical scans enable identification of any structural abnormalities that might be present, while functional scans provide useful information about neural activity. This information is especially helpful in the absence of any structural irregularities, which would explain the atypical brain function. Slices (two-dimensional cross-sections) of functional and structural MRI scans are shown in Figure 1. The structural image has noticeably higher spatial resolution. In fMRI, the voxel size

is limited by the tradeoff between small voxel dimension and high signal-to-noise ratio (SNR) [5]; however, even with this constraint, the spatial resolution of fMRI is still relatively high – on the order of a few millimeters. The temporal resolution of fMRI in human studies is generally in the range of one to three seconds per three-dimensional image. It is constrained by the necessity of using relatively low magnetic field strengths for safety purposes. The higher field strengths used in animal studies have resulted in temporal resolutions of 100 milliseconds.

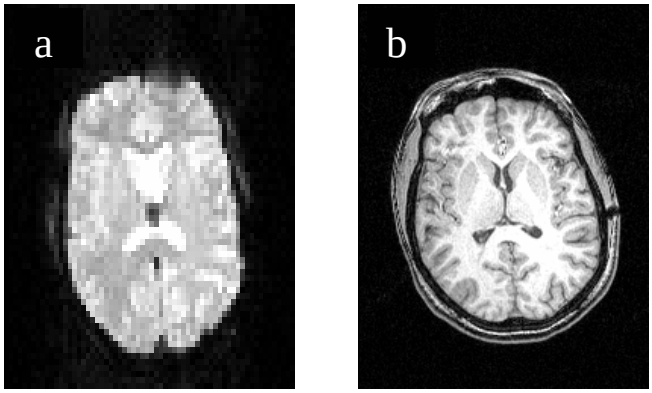

Figure 1. Examples of functional (a) and anatomical (b) images.

Functional MRI indirectly measures neural activity through detection of changes in blood flow, blood volume, and oxygen consumption. As regional brain function increases, there is a corresponding increase in regional cerebral blood flow (CBF). Blood oxygen level dependent (BOLD) fMRI exploits changes in concentrations of oxy- and deoxyhemoglobin that accompany changes in neural activity. The differences in the magnetic properties of these substances provide contrast in BOLD images. Arterial spin labeling (ASL) perfusion fMRI contrast is also a reflection of blood flow changes. During ASL perfusion scans, arterial blood water near the area of interest is electromagnetically labeled by a radiofrequency pulse to allow tracking of the CBF. Immediately after imaging of the pre-labeled spins, control images without labeled spins are

acquired. Through pairwise subtraction of these label and control pairs, the effects of labeling can be determined.

Table 1, as presented by Detre and Wang in [6], lists several properties of BOLD and ASL perfusion fMRI. BOLD fMRI generally has higher SNR and temporal resolution and larger signal changes due to activation than ASL perfusion. BOLD contrast is also easier to measure, so it is the more widely used technique. Despite the drawbacks mentioned, ASL perfusion contrast has characteristics that make it useful as well. The ASL imaging approach provides physiological measures of CBF, while the BOLD technique only provides information about relative changes in the blood oxygen. ASL also has the ability to measure resting function, which cannot be easily observed with BOLD contrast.

Table 1: Comparison of the properties of BOLD and ASL Perfusion fMRI [6].

	BOLD	ASL perfusion
Signal mechanism	Blood flow, blood volume, oxygenation consumption	Blood flow
Contrast parameter	T2*	T1
Spatial specificity	Venules and draining veins	Capillaries, arterioles
Typical signal change	0.5–5%	<1%
Imaging methods	Gradient-echo Offset spin-echo	Gradient-echo Spin-echo
Optimal task frequency (block design)	0.01–0.06 Hz	<0.01 Hz
Sample rate (TR)	1–3 s per image	3–8 s per perfusion image
Relative contrast-to-noise ratio	>2 with high task frequency <0.5 with low task frequency	1
Intersubject variability	High	Low
Imaging coverage	Whole brain	Part or most of brain cortex
Major artifacts	Susceptibility; motion; baseline drift	Vascular artifact

A major application of fMRI is the study of task-related functional activation. In these studies, the subject performs a specified task during scanning to locate the area of the brain responsible for that activity. For example, a subject might perform a finger tapping exercise in the scanner to image the brain regions involved in that activity. The most commonly applied experimental paradigms in the examination of task-related fMRI activation are block and event-related designs. Block designs involve trials of alternating periods of task and control conditions

to evoke sustained functional responses. The control blocks are designed to induce the same responses as the task stimuli, except for the cognitive process of interest. The differences between the responses to these two conditions can then be attributed to the task. Block designs maximize sensitivity by generating large, sustained signal changes, but individual tasks responses cannot be isolated with this type of experimental design. Conversely, event-related designs are devised to study responses to individual task stimuli and allow the activation due to these stimuli to be isolated. The difficulty with event-related studies is that statistical analysis of such data requires an accurate model of the hemodynamic response, which is not easily characterized [5]. Block data analysis is not as dependent on an accurate hemodynamic model.

2.2 Electroencephalography

Electroencephalography is a neurophysiologic tool for measuring electrical activity in the brain. The resulting recordings, known as electroencephalograms (EEGs), have high temporal resolution – on the order of milliseconds – compared to fMRI. Although neuroimaging methods, such as fMRI and positron emission tomography (PET), are increasingly utilized in the study of epilepsy, EEG continues to be the primary means of diagnosing and studying epilepsy syndromes.

During EEG recordings, electrical activity is measured through scalp electrodes, grid or strip electrodes placed directly on the cerebral cortex, or depth electrodes inserted into the brain. While scalp EEG is valuable because it is noninvasive, it suffers from low spatial resolution and is highly susceptible to motion and recording artifacts. Scalp EEG has an effective monitoring depth of only about 1 cm from the surface of the brain. The recorded signals are distorted and have much of their high frequency activity filtered out by the intervening tissue, skull, and cerebrospinal fluid. The inverse problem (i.e., using distant scalp electrodes to pinpoint distinct

generators of epileptic events) makes precise localization of the epileptic cortex impossible [7]. In contrast, intracranial EEG (IEEG) signals are relatively free of artifacts and easier to interpret than the noisy scalp traces. Another advantage of using intracranial electrodes is that they can be inserted directly into subcortical regions, such as the mesial temporal lobe, to observe areas at depths greater than 1 cm from the surface. IEEG often detects neural activity that is not visible or well localized in scalp recordings [8]. IEEG is clearly a more powerful tool in the study of epilepsy, but the collection of IEEG data is limited because of its highly invasive nature and the potential for surgical complications.

2.3 Applications of fMRI in Epilepsy Research

A potential complication of temporal lobectomy is the loss of memory and language functions. The intracarotid amobarbital test (IAT), also known as the Wada test, is the standard diagnostic tool for presurgical lateralization of memory and language. During the test, portions of one brain hemisphere are anesthetized so that function in the other hemisphere can be tested independently. Though this test is highly accurate, it is invasive and therefore potentially risky. Many researchers have investigated the application of fMRI as a noninvasive alternative to IAT. Desmond et al. [9] and Binder et al. [10] both reported strong agreement between the language laterality determined using fMRI and IAT on epilepsy patients. These studies involved using different tasks to activate regions of the brain responsible for language function in order to lateralize language dominance. Detre et al. performed a visual scene encoding task activation study for lateralizing memory function and also found excellent agreement between the fMRI and IAT results [11].

Detre et al. were able to detect localized signal intensity changes in the BOLD fMRI time courses of a focal epilepsy patient [12]. After subtracting the mean brain voxel intensity over the

12-minute scan from each slice, the images were thresholded to locate areas of significant functional change. Thresholds of 0.6 to 3% change from the mean were used. Through this time series analysis, they identified focal fluctuations that correlated well with the epileptogenic zones found using ictal SPECT (single photon emission computed tomography) and intracranial EEG. Subsequent region of interest analysis found two highly stereotyped events indicative of subclinical seizures. Though this method proved useful for mapping ictal activity with fMRI in this single patient, a larger study would be needed to validate the analysis. Also, a technique for identifying interictal activity would be even more advantageous since ictal activity during fMRI scans is uncommon and can result in large movement artifacts in the images.

Morgan et al. investigated the use of temporal clustering analysis (TCA) to localize interictal epileptic activity in resting BOLD images without the need for simultaneous EEG recordings [3]. They studied six temporal lobe epilepsy (TLE) patients and three patients whose seizure localization had not yet been confirmed by successful surgery. A histogram of the number of voxels reaching their maximum intensities at each point in time was created for each subject. Only voxels whose intensities were above a certain background noise threshold and whose maximum values were 2 to 10% greater than the initial intensity were include in the analysis. Peaks in the histogram were identified as time points with at least 100 voxels attaining a maximum intensity. These peaks found using TCA were then convolved with a BOLD hemodynamic response function to create a model of the BOLD signal response curve for that data series. Traditional event-related statistical parametric mapping (SPM) analysis, which involves application of the general linear model for statistical analysis of brain activity, was then carried out on the modeled BOLD response curves to find the areas of activation. The regions of activation found using TCA and SPM were concordant with the abnormal regions identified

using standard EEG and PET analysis. While the results are promising, the problem with the TCA technique is that spikes cannot be conclusively coupled with epileptic events since there are no electrophysiological recordings with which to correlate the spikes. Also, the peaks in the histogram are not necessarily due to epileptic activity. In fact, this technique incorrectly considers voxels randomly reaching their maxima during a peak to be activated.

Wolf et al. were able to detect mesial temporal lobe hypoperfusion in epilepsy patients using ASL perfusion data [13]. Twelve patients with medically refractory TLE and twelve healthy subjects were scanned using continuous ASL perfusion. Using manually drawn masks of the mesial temporal lobes (mTLs), the mean CBF values in those regions were calculated. The authors found that in the control participants, the normalized mTL CBF (found by dividing the regional mean by the global CBF) tended to be significantly higher on the left than the right side. There was evidence of hypoperfusion ipsilateral to (i.e., on the same side as) the epileptogenic temporal lobe in eleven of the twelve patients. Asymmetry indices – measures of the differences in the mean values between the two lobes – were not significantly different in patients and controls, but the asymmetry index proved useful in clinical lateralization. The ASL perfusion lateralization agreed with the PET lateralization for all but one patient who underwent an ^{18}FDG-PET scan. These results demonstrate that clinical lateralization of TLE patients can, in most cases, be determined by the presence of hypoperfusion in the ipsilateral mTL.

2.4 Combining EEG and fMRI

The use of both EEG and fMRI in the localization of epileptiform activity allows one to combine the high temporal resolution of EEG and the high spatial resolution of fMRI for a better understanding of the spatiotemporal dynamics of epileptiform discharges. This fusion provides the ability to correlate regional fMRI signal changes to epileptic spikes in the EEG. The

technical problems of acquiring simultaneous EEG and fMRI have been solved, and the data can be safely acquired using specialized equipment [14]. The use of MR-compatible electrodes, safety resistors, and fiber optic isolation protects the patient, and shielding the electronics minimizes the effects of the EEG recording on the image quality. A more difficult problem to address is the creation of large artifacts in the EEG signal during simultaneous image acquisition. The voltages of the time-varying magnetic fields completely obscure the EEG rendering the data useless in the absence of any post-processing. For this reason, most EEG/fMRI recordings have been interleaved until recently.

Jäger et al. developed a spike-related fMRI method to detect epileptiform activity [15]. The EEG recordings were monitored online by a neurologist, and BOLD fMRI recordings were initiated 3–5 seconds after an epileptic discharge. The image acquisition was delayed to ensure that EEG events did not influence image contrast. There is an approximately three second delay in BOLD signal changes after an event, so the imaging delay did not result in the loss of contrast data after the EEG event. Ballistocardiographic contamination, artifacts in the EEG due to the beating of the heart, was removed using subtraction techniques, and artifacts that arose due to imaging were removed using commercially available software. The authors were able to find significant increases in the BOLD signal intensity, with a peak 6–7 seconds after the spike detection. The signal then decreased and returned to normal after about eighteen seconds. These results are promising for understanding the hemodynamic response to interictal events, but the problem with this technique is the lack of baseline imaging data and pre- and post-ictal data. Continuous, simultaneous EEG and fMRI recordings clearly provide more useful information.

With more advanced hardware and improved post-processing techniques for imaging artifact removal, continuous acquisition of both functional MR images and EEG is now possible

[16]. Bénar et al. discuss various techniques for the removal of the ballistocardiogram and gradient artifacts from the EEG. Previously subtraction techniques and spatial filtering had been used to eliminate the ballistocardiogram. Here the authors present spatial filtering techniques based on principal component analysis (PCA) and independent component analysis (ICA). When spatially filtering, there is a tradeoff between removing the ballistocardiogram and preserving the spikes in the EEG. When using PCA decomposition, ballistocardiographic activity is usually clearly visible in one or two components. By removing one component, they found the best results in terms of balancing removal of the ballistocardiogram and preservation of the spikes. With ICA there is typically clear ballistocardiographic activity in three or four components, which can all be removed while preserving spikes. Spatial filtering using ICA tended to yield better results than PCA.

Bénar et al. also developed a technique for removing the gradient artifact [16]. The procedure entailed building a model of the artifact and subtracting it from each frame of the EEG. They compared their technique to the Fourier method developed by Hoffmann et al. in [17] and found that their subtraction filter worked better than the Fourier method in most cases and worked as well in all other cases. The Fourier method involved computing the FFT of 10-second segments of EEG and noting frequencies for which the FFT amplitude differed from the baseline spectrum by more than a certain factor (typically two or three). The corresponding Fourier coefficients of these frequencies were set to zero and an inverse Fourier transformation was obtained, thus yielding a signal that was free of artifacts.

Baudewig et al. were able to localize epileptic activity by linking EEG abnormalities to BOLD signal changes in simultaneously recorded fMRI [18]. In their study, an epileptologist examined the EEG and identified segments of epileptic activity. The epileptic events were then

correlated with specific images. For each of these images, they measured the change in BOLD signal intensity in order to find the activated pixels in each image. One unresolved problem with their work and all BOLD fMRI analysis is whether the areas of epileptic activity found were the true epileptic foci or simply areas of induced activity.

Combining EEG and fMRI in the localization of epileptiform generators appears quite promising, but the equipment necessary to acquire simultaneous EEG and fMRI data is not widely available. Until such resources become available, another option for fusing the two modalities is to examine EEG and fMRI data acquired from the same patient at different times and correlating the areas of fMRI activation with the EEG channels exhibiting epileptic spikes. While such an analysis would not be as powerful as studying simultaneous recordings, it would likely prove to be more accurate than analysis of fMRI alone.

2.5 Genetic Programming

Genetic programming (GP) is a machine learning technique that employs an evolutionary algorithm to generate an optimal program to solve a given problem [19, 20]. Evolutionary algorithms apply genetic operators such as reproduction, mutation, crossover, and selection to find optimal solutions from populations of candidate solutions, also known as individuals or chromosomes. Individuals are assessed through evaluation of a fitness function, which measures the individual's ability to solve the given problem. The result of the algorithm is the individual with the best fitness.

GP is an extension of genetic algorithms (GA), but there are a few key differences. First, unlike GA, which finds a direct solution to a problem, GP outputs a program that can be used to solve the problem. The variably sized GP programs are represented as tree structures; on the other hand, GA chromosomes are fixed-length and represented as strings or vectors of binary or

real values. Because the size of individuals is not fixed in GP, the algorithm is capable of creating both simple and highly complex individuals. A simple example a GP tree is shown in Figure 2. The gray nodes represent functions, and the white nodes represent terminals. Functions are arithmetic, mathematical, Boolean, or conditional operators, and terminals are user inputs to the GP algorithm and constants.

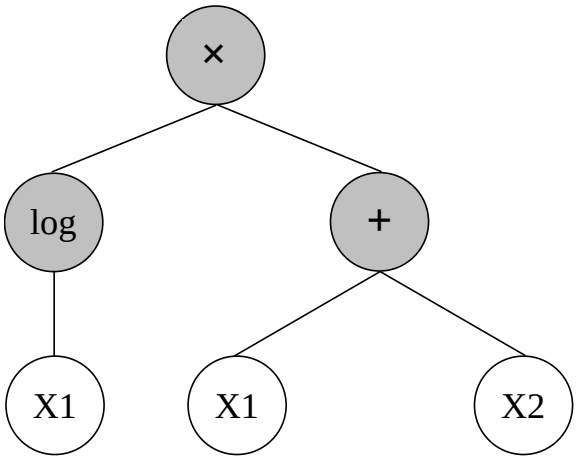

Figure 2. Tree representation of the GP program log(X1)×(X1+X2).

The GP algorithm evolves programs through an iterative process. Each iteration of the algorithm is known as a generation. During the initial generation, randomly generated individuals populate the solution space. With each new generation, the population is diversified through selection, crossover, and mutation operations. Selection involves choosing a set of individuals from the larger population based on a fitness criterion. In a crossover operation, two new individuals (offspring) are produced as combinations of two parents. This is accomplished by selecting a node in each parent tree and then swapping the subtrees branching from those nodes. Figure 3 illustrates a typical crossover operation. Like crossover, mutation operations generate new offspring; however, mutation involves only a single parent. A subtree is selected

and replaced by a randomly generated tree to create a new individual. A mutation operation is illustrated in Figure 4. The process of creating new populations continues until the maximum number of generations is reached or until a stop criterion, such as a specified fitness level, is met.

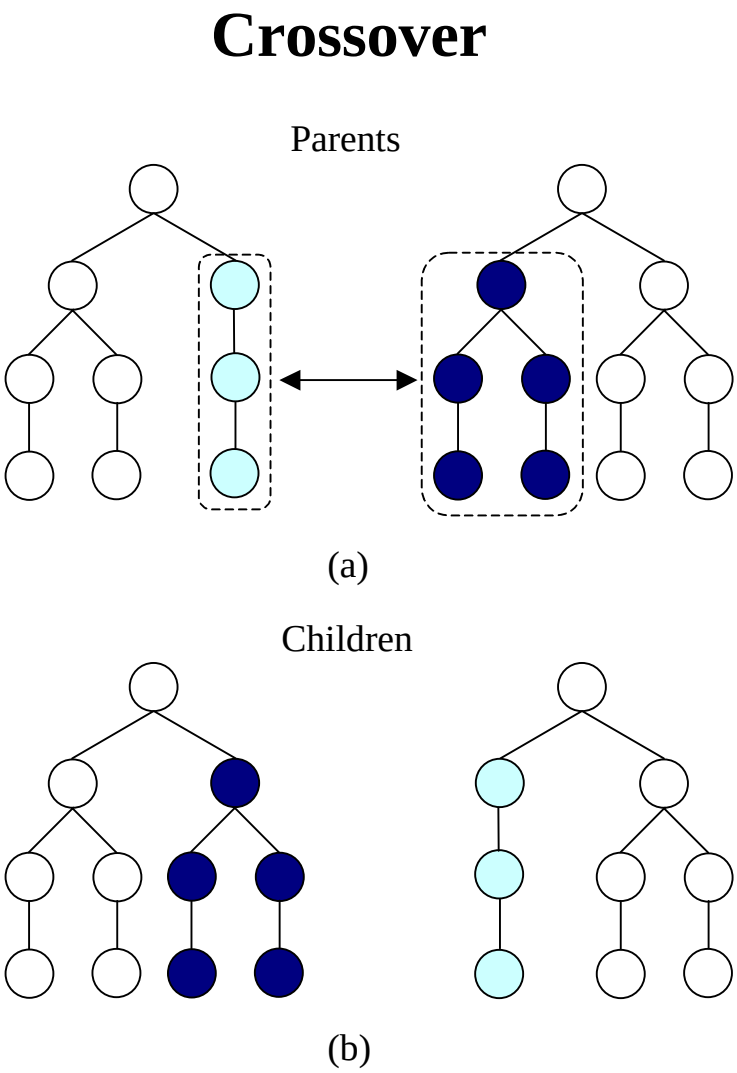

Figure 3. Illustration of a GP crossover operation. (a) Individuals whose subtrees will be swapped. (b) The new individuals resulting from the crossover.

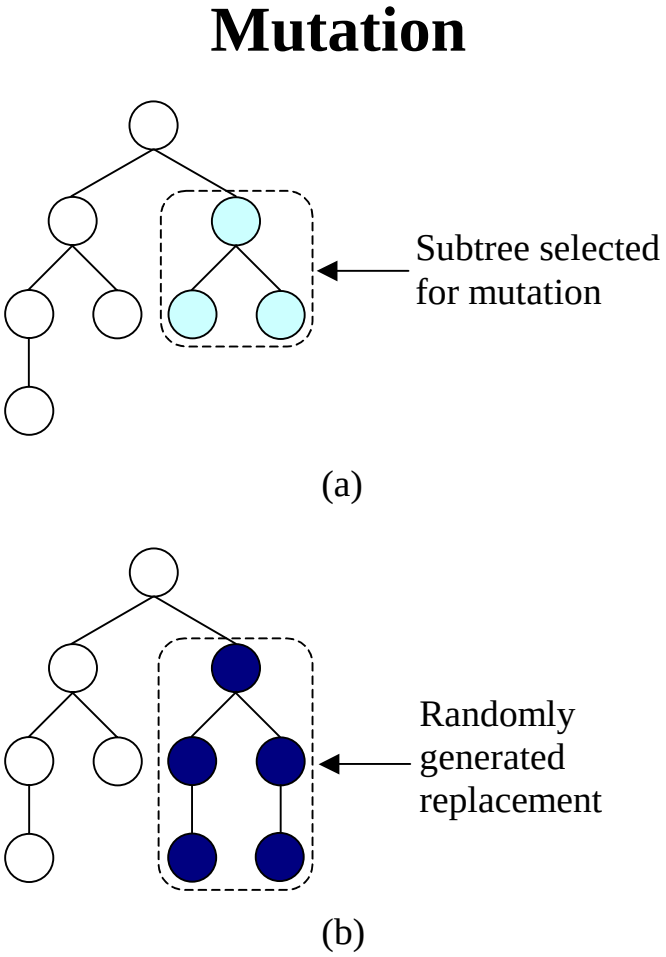

Figure 4. Illustration of a GP mutation operation. (a) Individual with subtree selected for mutation. (b) New individual created through mutation.

3 Preliminary Research

3.1 BOLD fMRI Analysis

Event-related BOLD data from eleven temporal lobe epilepsy (TLE) patients were acquired from the Center for Functional Neuroimaging at the University of Pennsylvania. Each event-related dataset consists of 298 three-dimensional image volumes acquired three seconds apart at a magnetic field strength of 3 Tesla. The raw images are $64 \times 64 \times 40$ voxels in size with a voxel resolution of $3 \times 3 \times 3$ mm^3. An example of a raw BOLD image is shown in Figure 5. From the group of eleven patients, the three who at the time of this analysis had been rendered seizure free by surgery were chosen for the initial investigation. For these patients, the seizure foci were correctly identified by their doctors and could be used to validate the results.

To ensure that the class separation found in the feature analysis was truly due to differences between the epileptic and normal regions, not simply intrinsic differences between the two brain hemispheres, control data from healthy subjects had to be analyzed as well. Unfortunately, no event-related BOLD data from controls were available. Although comparisons of data acquired using different experimental paradigms are not ideal, block scans from one normal subject were evaluated to compare with the patients' results. Both the block and event-related paradigms were designed to activate the mesial temporal lobe for memory lateralization. The block design as described in [21] involved presentation of complex visual scenes and a single control image in alternating forty-second blocks. A single visual stimulus was presented approximately every fourteen seconds for the event-related design. The block dataset consists of 172 fMRI images of the same size, temporal spacing, and magnetic field strength as the event data.

Figure 5. A single raw BOLD image of a patient with temporal lobe epilepsy.

In the following sections on BOLD fMRI analysis, the three patients will be identified as S5, S6, and S11, and the healthy control will be referred to as C1.

3.1.1 Preprocessing

Before the images could be analyzed, they had to be preprocessed to reduce artifacts and noise corruption. The first four images from each set of scans were discarded because the magnetization had not yet stabilized to a steady state. The remaining images were then realigned to the first functional image in order to account for signal changes due to subject motion during scanning [22]. Following realignment, the functional and anatomical images were co-registered so that they lined up evenly with one another. As every brain has unique shape, size, and

structure, all scans were subsequently normalized to a $3 \times 3 \times 3$ mm^3 Montreal Neurological Institute (MNI) template for comparison across patients. Normalization warps images so that they conform to the space of a standard template brain [22]. The resulting dimensions of the normalized images were $53 \times 63 \times 46$ voxels. The final step before signal analysis was spatial smoothing. A seven-millimeter full width at half maximum Gaussian smoothing kernel was applied to increase the overall signal-to-noise ratio (SNR), while also limiting the low-frequency noise amplification caused by spatial smoothing with too large a kernel [23]. All realignment, co-registration, normalization, and smoothing were performed with Statistical Parametric Mapping software (SPM2) [22, 24, 25].

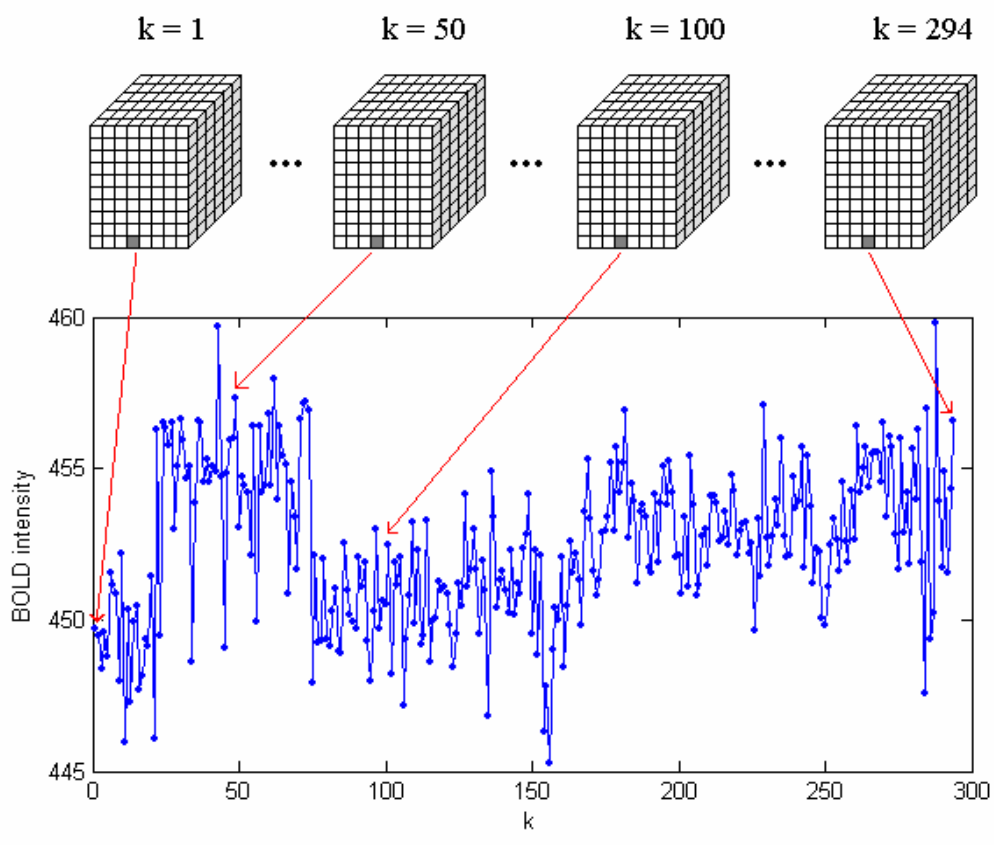

Figure 6. BOLD signal time course extraction.

3.1.2 Time Course Extraction

The voxel time course is a signal corresponding to the change in a voxel's intensity throughout time. Each image is a three-dimensional array representing the fMRI signal values of the voxels at a single point in time. By extracting the voxel intensity from the images at every time point, the voxel time course can be obtained as shown in Figure 6.

The considerable size of the final preprocessed images makes analysis of all voxels extremely computationally expensive. To reduce the total amount of data being processed, region of interest (ROI) analysis was employed. Masks of each mesial temporal lobe, consisting of the hippocampus, amygdala, and parahippocampal gyrus, were created using the WFU Pickatlas toolbox for SPM2 [26-28], which allows users to generate and save anatomical masks using a set of human brain atlases. These standardized masks were the bases for the subsequent regional analyses.

3.1.3 Feature Extraction

In the absence of any structural abnormalities, the epileptic focus cannot be identified simply through visual inspection of anatomical or functional images. Figure 7 shows the BOLD time courses of voxels from the left and right mesial temporal lobes of a TLE patient with left side onset. The differences in the time courses of the voxels from the two hemispheres do not visibly indicate which region is normal and which is epileptogenic. Clearly, a quantitative analysis technique is needed to lateralize TLE.

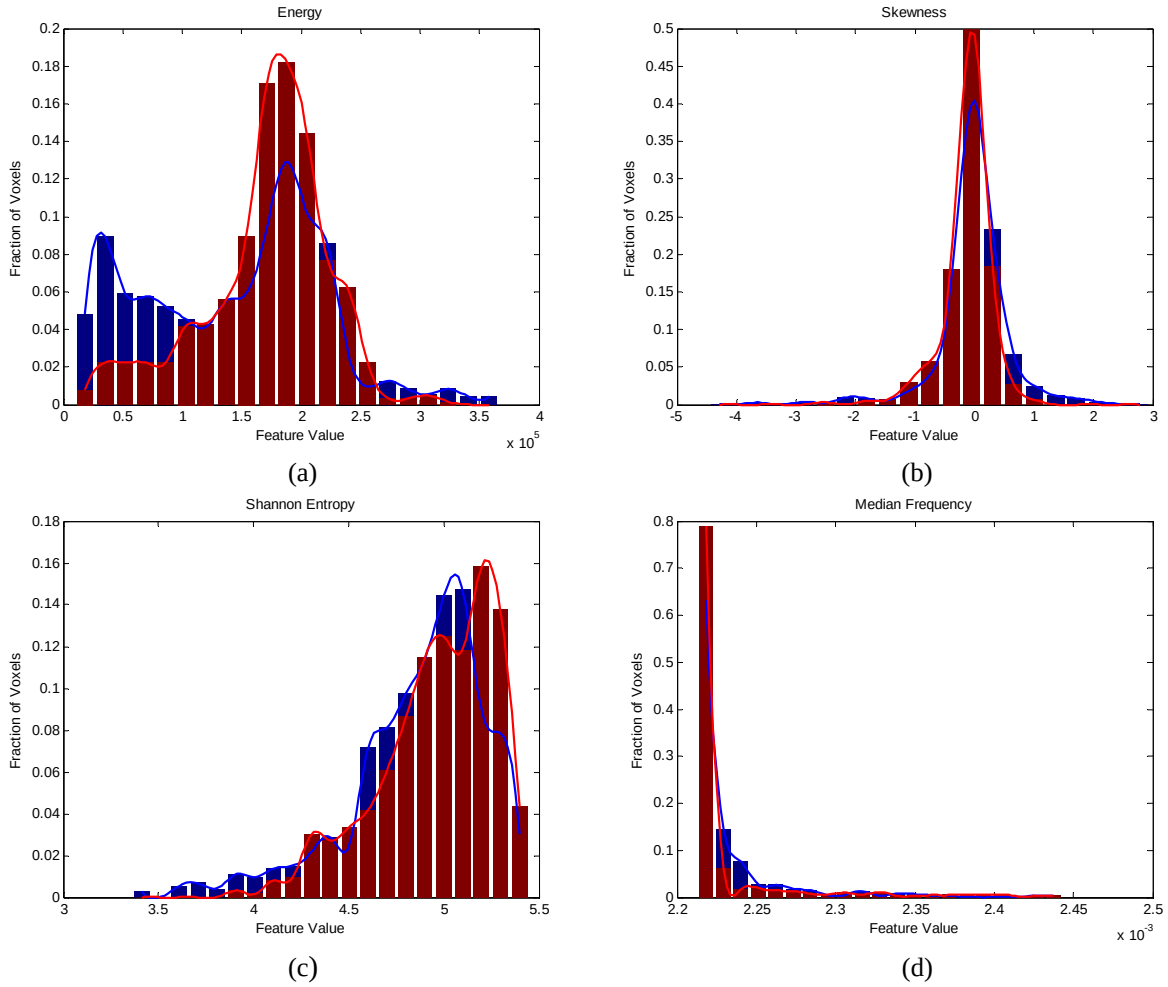

Figure 7. Normalized histograms of feature values for patient S5. (a) Energy, (b) Skewness, (c) Shannon Entropy, (d) Median Frequency. Blue denotes the left mTL, and red denotes the right mTL.

The thirteen features listed in Table 2 were extracted from the time courses of the mesial temporal lobe voxels to determine which, if any, would be useful in differentiating between the normal and abnormal lobes. These features were chosen because they made intuitive sense and because they have proven useful in the analysis of other electrophysiological signals such as EEG [29]. Features from multiple domains were extracted to reveal not only temporal characteristics of the time courses but frequency and statistical information as well. The time domain features, energy, curve length, and nonlinear (Teager) energy measure signal strength and variability between successive samples. The median, mean, and peak frequency values

correspond to the frequencies at which the power spectrum of a signal reaches its median, mean, and peak, respectively. Shannon entropy measures the randomness in the amplitude of the signal, whereas spectral entropy measures the randomness in the distribution of frequency in the power spectrum. Renyi entropy is a generalization of Shannon entropy, and the statistical features convey information about the probability distributions of the signals. In the presence of epileptiform discharges, one might expect higher signal amplitudes and greater oscillations in the BOLD signal due to the increased neuronal activity. The previously described features seem suited to identifying such signal changes.

3.1.4 Genetic Programming

None of the thirteen features extracted from the data showed clear separation between the left and right mesial temporal lobes. In most cases the histograms of the feature values for the two classes overlapped almost completely. Figure 8 shows the histograms of four features extracted from the BOLD time course of patient S5. The blue PDF denotes the left mTL feature values, and the red denotes the right mTL values. The other features had similar distributions.

Genetic programming was employed to fuse the various features into one for better class separation for each patient. The thirteen feature values from all mTL voxels were entered into the GP. The GP was allowed to evolve over one hundred generations to find the program that would minimize the fitness function. The inverse of the Fisher discriminant ratio (IFDR), seen in equation 1, was chosen as the fitness function because it measures class separability, and the goal was to maximize the distance between the two classes. The patient-specific features created by the GP when applying this fitness function were quite complicated and non-intuitive. At times, the trees grew to over two hundred nodes before reaching the maximum number of

generations. Such complexity suggests that the GP algorithm is modeling fMRI noise, not the underlying hemodynamic response.

Table 2. Feature Set.

Domain	Feature	Formula
Time	Energy	$\sum_i x_i^2$
	Curve Length	$\sum_i \lvert x_i - x_{i-1} \rvert$
	Nonlinear (Teager) Energy	$\sum \left(x_i^2 - x_{i+1} \cdot x_{i-1} \right)$
Statistical	Mean	$\frac{1}{N} \sum_i x_i$
	Variance	$\frac{1}{N} \sum_i (x_i - \mu)^2$
	Skewness	$\frac{1}{N} \sum_i \left(\frac{x_i - \mu}{\sigma} \right)^3$
	Kurtosis	$\frac{1}{N} \sum_i \left(\frac{x_i - \mu}{\sigma} \right)^4$
Mutual Information	Spectral Entropy	$-\sum_i P_{xx} \times \log_2(P_{xx})$
	Shannon Entropy	$-\sum_i p_i \times \log_2(p_i)$
	Renyi Entropy	$\frac{1}{1-q} \log_2 \sum_i p_i^q$
Frequency	Median Frequency	$\frac{index(median(P_{XX})) - 1}{length(P_{XX}) - 1} \times \frac{F_S}{2}$
	Mean Frequency	$\frac{index(mean(P_{XX})) - 1}{length(P_{XX}) - 1} \times \frac{F_S}{2}$
	Peak Frequency	$\frac{index(\max(P_{XX})) - 1}{length(P_{XX}) - 1} \times \frac{F_S}{2}$

Note: μ = mean of x, P_{xx} = power spectral density of x, p = histogram of x, F_s = sampling frequency.

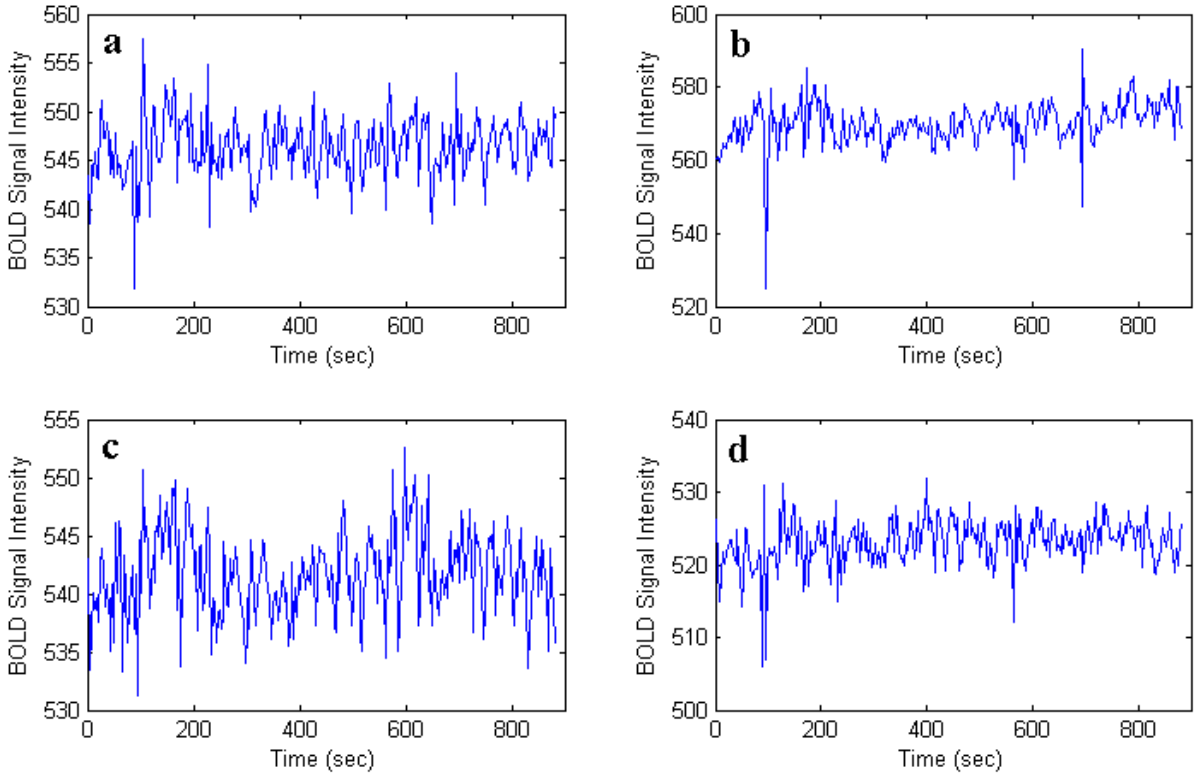

Figure 8. Time courses of mesial temporal lobe (mTL) voxels of a TLE patient. (a,b) Left mTL voxels from slices 14 and 16, respectively. (c,d) Right mTL voxels from the same slices.

$$IFDR = \frac{\sqrt{\sigma_1^2 + \sigma_2^2}}{|\mu_1 - \mu_2|} \tag{1}$$

An example of a GP tree is shown in Figure 9. The terminal nodes, represented by dots, are the input features listed in Table 2. The GP routine assigned a label, X1 – X13, to each feature for graphical representation. The triangles in the tree structure represent operators from the function set used to create the best individual. The function set consists of built-in Matlab functions and user-defined functions.

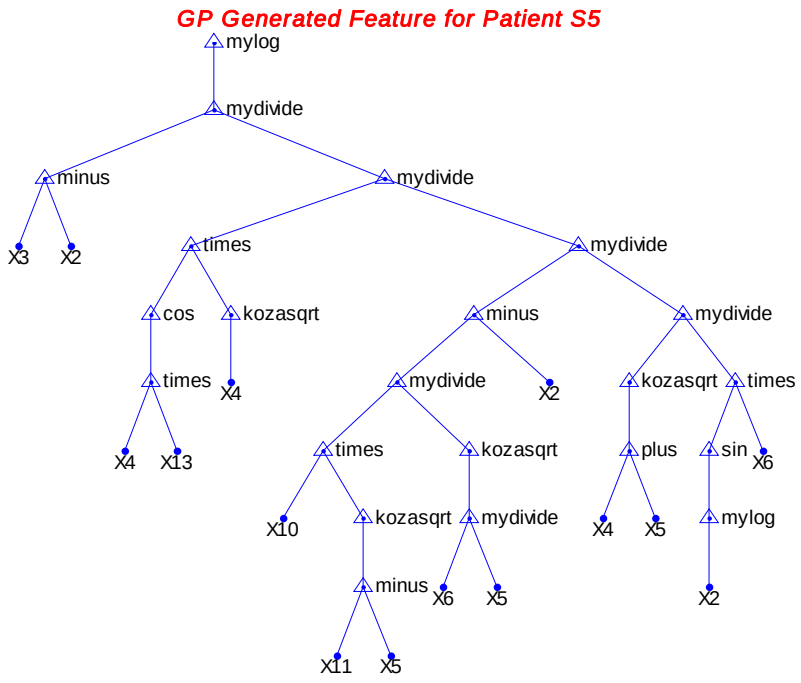

Figure 9. Tree representation of composite feature generated by the GP for patient S5.

3.1.5 Classification

The results of the GP were assessed qualitatively through visual inspection of the resulting feature histograms and also by classification accuracy. In all cases, the composite features still resulted in significant overlap between the two classes, so the classifier-based measure of separability was needed to determine the usefulness of these composite features. A k-nearest neighbor (k-NN) classifier (k = 3) was applied to label all voxels as belonging to either the left or right mTL. The classification accuracies when using the GP generated features were similar in the patients and control. All accuracies were in the range of 75 – 86%, where the lower values resulted from the analyses of patient S6 and control C1. From these classification accuracies, it is evident that this GP based feature creation technique can detect differences between voxels in the left and right brain hemispheres of epilepsy patients and healthy controls;

however, the nature of these differences is not clear. They could be due to the presence of epileptic activity, or they could result from normal variations in each subject's brain regions.

3.1.6 Noise Removal

In addition to spatially smoothing the images to increase SNR, linear detrending and principal component analysis (PCA) and independent component analysis (ICA) based noise removal techniques and were applied to the data for noise reduction. Linear detrending was applied to remove low frequency signal drift, which can overshadow activation [30]. Thomas et al. investigated the use of component analysis to separate BOLD signal change from random noise [31]. To reduce the random noise, time courses were decomposed using both PCA and ICA, and those components determined to be mainly white noise were set to zero. The signals were then reconstructed from the remaining components and analyzed again. While the noise removal techniques did improve the overall SNR of the time courses, they did little to improve the classification accuracy for any of the subjects. Physiological noise resulting from respiratory and cardiac effects could still be hindering with the analysis. This difficulty in clearly discriminating between normal and epileptic activity could be due to the BOLD signal contrast's inability to detect slow changes in neural activity over long periods of time [32]. Although the majority of the event-related images were taken during rest, the task activation may still have overshadowed the response due to epileptiform discharges.

3.2 ASL Perfusion fMRI Analysis

Continuous ASL (CASL) perfusion datasets from three epilepsy patients and two control subjects were studied to determine whether or not perfusion fMRI data are better suited than BOLD fMRI to imaging blood flow changes due to spontaneous neural activity in epileptic networks. The resting perfusion images were collected during consecutive ten-minute scanning

sessions at 3T with a repetition time of three seconds. All subjects, except the first control, were scanned for forty minutes, so these datasets consist of four functional runs and contain a total of 800 images. The first control dataset consists of only two functional runs. The raw perfusion images are $64 \times 64 \times 16$ arrays with voxel resolutions of $3.44 \times 3.44 \times 7.50$ mm^3. The odd numbered scans are label images, and the even numbered scans are control images.

3.2.1 Preprocessing

A slightly different preprocessing approach was adopted in preparing the perfusion data for analysis than was taken with the BOLD data. This procedure was chosen in conjunction with functional imaging researchers at the University of Pennsylvania. Instead of realigning whole images to one another, the images were realigned slice-by-slice to reduce artifacts in the final cerebral blood flow (CBF) images. The images were then smoothed with an 8 mm full width at half maximum Gaussian kernel to reduce noise. After smoothing, the functional and anatomical images were co-registered.

3.2.2 Perfusion Signal and CBF Calculation

One of the advantages of ASL perfusion over BOLD is that it measures blood flow changes in physiological units of ml/100g/min unlike BOLD fMRI, which can only measure relative changes in local blood oxygenation. The raw output images of ASL perfusion scanning must be converted into CBF images to measure blood flow. The perfusion images were created through simple pairwise subtraction, meaning each label image was subtracted from the preceding control image. The CBF images were then calculated from the perfusion images using the equation described in [33].

The first step in our image analysis was to look for evidence of hypoperfusion in the epileptogenic lobes similar to that found by Wolf et al. [13]. Patients 1 and 3 showed

hypoperfusion in both the epileptogenic mTL and the entire temporal lobe. Patient 2 did not exhibit hypoperfusion in the epileptogenic mTL but did within the whole temporal lobe. There were also perfusion asymmetries between the two hemispheres in the controls. In both cases, the right mTL had a lower perfusion value than the left, as reported by Wolf et al. For all patients, neurologists determined the seizure onset side through analysis of EEG recordings. The mean CBF calculations are summarized in Table 3.

Table 3. Mean CBF values (in units of ml/100g/min) over the entire scan time.

Subject	Seizure Side	Global	Mesial Temporal Lobe		Temporal Lobe	
			Left	Right	Left	Right
Pt1	Left	70.322	78.171	83.930	89.875	96.847
Pt2	Right	45.667	58.568	61.689	66.331	62.739
Pt3	Left	27.768	47.477	52.852	52.023	58.713
Control1	N/A	56.136	78.152	74.882	91.148	92.566
Control2	N/A	42.543	48.952	47.459	56.988	58.390

3.2.3 Feature Extraction and Fusion

The features listed in Table 2 were extracted from the time courses of the mesial temporal voxels of the CBF images. For the preliminary analysis, only images from the final ten minutes of the functional scans were analyzed because by that time all subjects had fallen asleep. There is generally increased epileptic activity in TLE patients during sleep, so these images likely contain abnormal activity. As before, the features were fused for each subject using a GP algorithm. In addition to the function described in equation 1, a new fitness function was tested. This fitness measure, found in equation 2, is the inverse Fisher discriminant ratio divided by one minus the PDF overlap. This fitness function was chosen because features with seemingly good fitness values may still have large overlaps. The overlap values range from 0 (no overlap) to 1 (total overlap). The new fitness function penalizes individuals with large class overlaps by increasing

the fitness score in proportion to the amount overlap. The individual with the lowest fitness score is ultimately selected.

$$fitness = \frac{\sqrt{\sigma_1^2 + \sigma_2^2}}{|\mu_1 - \mu_2|} \times \left(\frac{1}{1 - \text{PDF overlap}}\right) \quad (2)$$

3.2.4 Classification

The GP generated features from the CBF time courses were also evaluated qualitatively and quantitatively. Two of the patients, Pt1 and Pt2, had composite features that showed good separation between the left and right mTLs. The third however, Pt3, had much larger areas of overlap in the feature histograms. The composite features for the two controls also overlapped significantly. The features generated using the fitness in equation 2 had higher accuracies than those found using equation 1, so equation 2 was selected as the better fitness function for this application and used in all analysis of the ASL data. The accuracies of the k-NN classifier and GP tree information for all subjects are summarized in Table 4. The overall accuracy, sensitivity, specificity, and the numbers of levels and nodes in the GP trees are included.

Table 4. ASL perfusion data classification results.

Subject	Accuracy	Sensitivity	Specificity	Levels	Nodes
Pt1	92.267%	90.439%	94.215%	5	8
Pt2	90.333%	94.574%	85.813%	9	15
Pt3	82.267%	79.845%	84.849%	7	14
Control1	75.400%	68.217%	83.058%	10	46
Control2	82.333%	76.486%	88.568%	10	48

The GP features when combined with a k-nn classifier were highly accurate in distinguishing between normal and epileptic mTLs in Pt1 and Pt2. The classification accuracy for Pt3 was decent but not as high as for the other two patients. Although the GP was able to separate the two classes to an extent in both controls, the features it generated were much more

complex than the patient features, meaning the GP could find distinctions between the two regions but with more difficulty. These dissimilarities could be attributable to noise or other physiological patterns unrelated to epileptic activity. As shown in Table 3, there are inherent differences in the mean CBF values of the left and right lobes. The GP may well be recognizing these intrinsic variations in the cases of the controls. On the other hand, the patients' mTLs have more easily characterized differences that can be encapsulated in simpler features.

3.2.5 Universal Features

While patient specific features are useful for analyzing data on a case-by-case basis, a universal feature, one applicable to all epilepsy patients, would be more powerful. After initial training of the GP and the classifier to find this universal feature, the feature extraction and genetic programming steps previously described would no longer be necessary. The universal feature would simply be extracted from the preprocessed data, and then all voxels would be classified based on this criterion. Patient specific feature generation was chosen for the previously described analysis because physiological differences between patients would likely confound universal feature creation.

In an attempt to find such a feature for the ASL perfusion data, the voxels from the epileptogenic and normal lobes of the two left TLE patients, Pt1 and Pt3, were entered into the GP to find a feature capable of separating the two classes. The resultant feature had a classification accuracy of 82%, but the GP tree consisted of thirty-seven nodes and nine levels. As previously discussed, this large tree size could indicate that the GP is finding random differences or innate physiological differences not associated with epileptic activity.

After being unable to find a good universal feature, the feasibility of creating one was tested. Voxel features from the left mTLs of Pt1 and Pt3 were compared to one another to

determine the amount similarity between them. The test was then repeated for the right mTLs. In both cases, the GP was able to separate the patients' voxels with over 99% accuracy using simple features with low numbers of nodes and levels. The GP tree and feature histogram for the right mTL voxels of Pt1 and Pt3 are shown in Figures 10 and 11, respectively. This result substantiates the initial hypothesis that physiological variations cause feature values across patients to be completely different and therefore not comparable. Because the time courses are so disparate, grouping voxels across patients to find commonalities is not possible, thus making creation of universal features impractical.

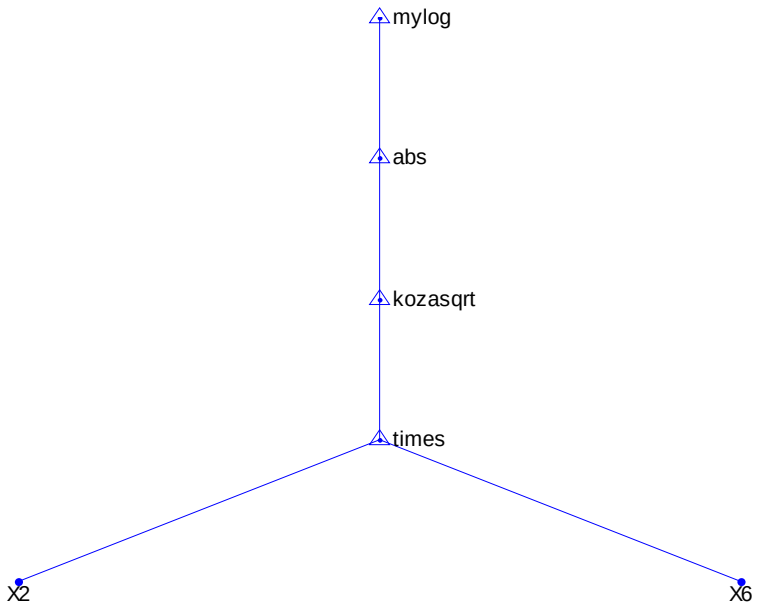

Figure 10. GP feature tree for separating right mTL voxels of Pt1 and Pt3.

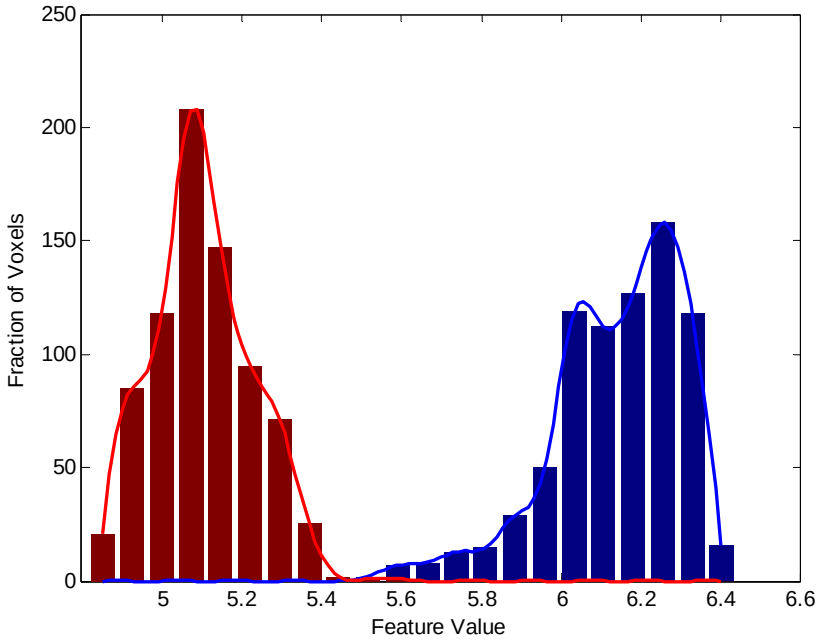

Figure 11. GP histogram corresponding to the feature in Figure 10. The blue and red represent Pt1 and Pt3 respectively.

SECTION II

4 Proposed Research

The objective of the proposed research is to develop a novel voxel-based analysis technique for mapping epileptic networks by distinguishing between normal brain tissue and the epileptic focus in fMRI data. Functional MRI is a noninvasive technology possessing higher spatial resolution than scalp EEG, which is typically used for focus localization. Accurate localization of the epileptogenic zone is crucial for successful outcome to surgery in patients with medically refractory epilepsy. As implantable neurostimulators become more widely used, correct localization will also be essential for placement of sensing and stimulation electrodes.

The primary objective will be addressed through the development and validation of a set of features from the time, frequency, information theory, and statistical domains that will enable clear discrimination between normal and abnormal brain tissue in the ASL perfusion images of temporal lobe epilepsy patients. Initially, the data will be preprocessed to account for artifacts due to subject motion during imaging, to increase the signal-to-noise ratio, and to normalize all data into a standard space for cross subject comparisons. Then, for each voxel in the regions of interest, features will be extracted from the voxel time courses, and these values will be entered into a genetic programming algorithm for fusion of the features and creation of a single composite feature for better class separation. The composite feature value will be the criterion used for classifying the voxels as either normal or epileptogenic.

The following section presents the proposed methodology in greater detail.

4.1 Proposed Methodology

The proposed methodology consists of five main components: preprocessing, time signal extraction, feature extraction, genetic programming, and classification. A block diagram of the system is shown in Figure 12.

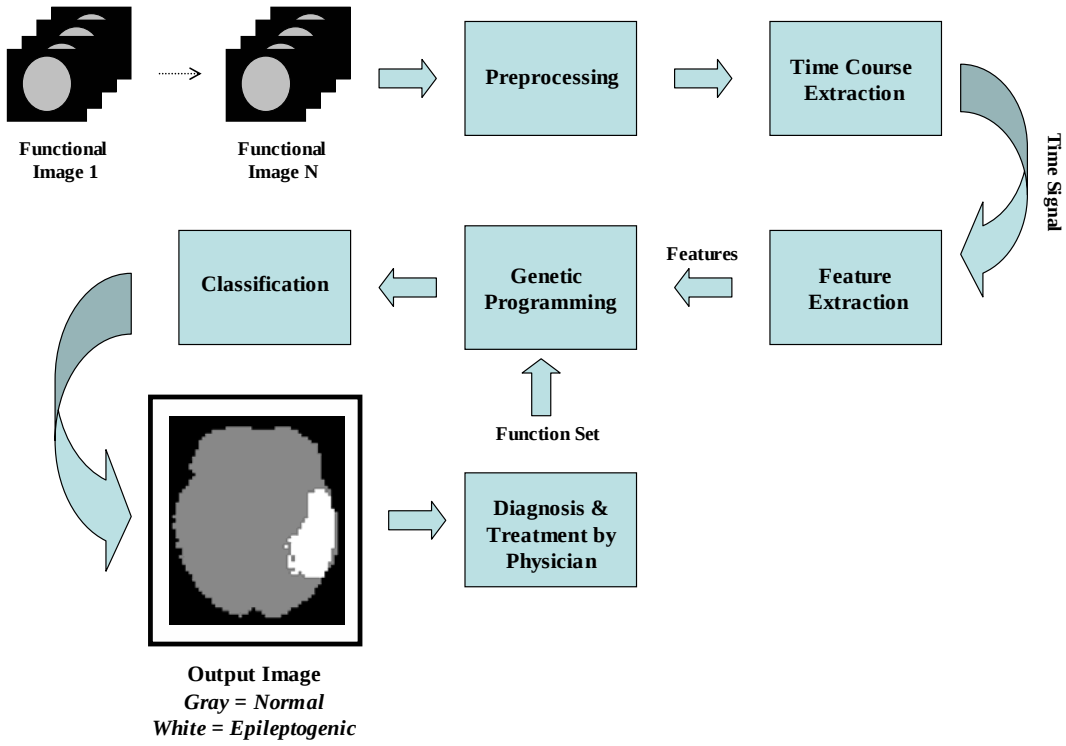

Figure 12. Proposed system for normal/epileptogenic tissue discrimination.

4.1.1 Data

Resting ASL perfusion data from approximately twenty temporal lobe epilepsy patients and ten controls will be collected by the Center for Functional Neuroimaging at the University of Pennsylvania over the next year and will be provided for analysis as it becomes available. Each subject's perfusion dataset consists of four consecutive ten-minute perfusion runs, and each ten-

minute run contains 200 images. The functional runs will be analyzed individually and also concatenated to see how blood flow changes evolve over longer periods of time in the epileptic brain. If any of the patients are implanted with intracranial electrodes in the near future, as expected, IEEG and fMRI localization results will be compared. Information about suspected seizure sources as determined by initial scalp EEG monitoring and PET scans will also be provided for all patients.

4.1.2 Preprocessing

Prior to any analysis of fMRI data, the images must be preprocessed to remove artifacts due to subject motion and scanner noise. For the ASL perfusion data to be analyzed, the preprocessing procedure includes realignment of the data to reduce motion artifacts, and spatial smoothing with a Gaussian kernel to average out uncorrelated noise. The data are also normalized to warp all scans into the space of a template brain so that cross patient comparisons can be made and standardized masks can be used for regional analysis. All of these steps will be carried out using the SPM2 toolbox for Matlab. Much of the scanner and physiological noise may still be present after the initial preprocessing, so additional measures, such as ICA or PCA based noise removal, may be necessary before individual voxel time courses can be examined and used for classification.

4.1.3 Voxel Time Course Extraction

Typically in epilepsy research, resting perfusion data are examined for the presence of hypoperfusion in the epileptogenic region. This entails computation of the mean CBF image over time and comparing the mean value within the suspected epileptic region and the corresponding contralateral region. The proposed research focuses on investigating how signals evolve over time in each individual voxel, not simply considering the mean value of each voxel.

Each normalized image consists of 153,594 voxels, so to reduce the computational burden, regions of interest (ROIs) are defined and become the focus of the investigation. Through the review of previous research in fMRI analysis and discussions with neurologists, multiple ROIs have been chosen for the temporal lobe epilepsy patient study. These regions include the entire temporal lobe, the mesial temporal lobe, and the hippocampus. Figure 13 shows a single slice of the masks for these three regions. ROI masks will be created using the WFU Pickatlas program. A neurologist will also draw patient specific masks for comparison purposes. As all brains are different, no template masks can perfectly match the structure of every individual's brain, even if the images have been transformed into a standard space. The patient specific masks will more accurately represent the ROIs and could potentially alter the results significantly.

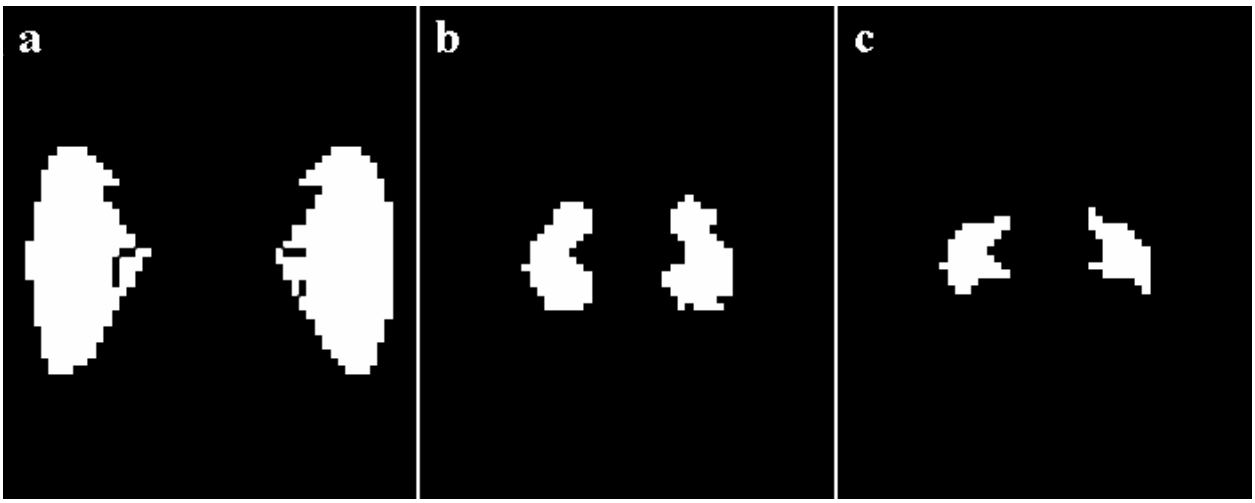

Figure 13. Slices from the normalized ROI masks of the (a) temporal lobe, (b) mesial temporal lobe, and (c) hippocampus.

4.1.4 Feature Extraction

Additional features must be investigated to find the best set for distinguishing between epileptogenic regions and normal tissue. Of the thirteen features examined thus far, no single

feature shows a clear distinction between normal and abnormal tissue. In most cases, the feature values in these two regions completely overlap. Through the exploration of additional features from the time, frequency, statistical, and mutual information domains, we hope to attain better class separation and therefore better classification results. Receiver operating characteristic (ROC) analysis will be used to assess the performance of the features. A receiver operating characteristic is a plot of the sensitivity versus one minus the specificity of a classifier as the discrimination threshold is varied. The area under the curve (AUC) indicates how well the classifier performs [34]. Random classification will result in an AUC of 0.5, and a perfect classifier will have an AUC of 1. Each features value as a predictor will be assessed based on its AUC. An example of an ROC curve is shown in Figure 14.

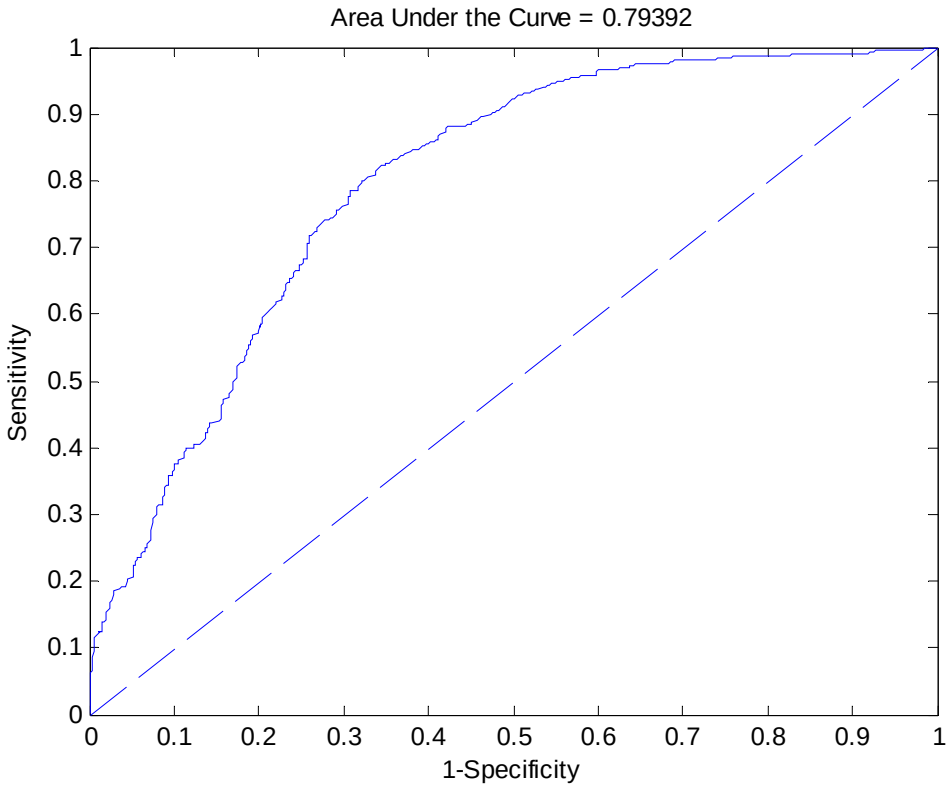

Figure 14. Examples of ROC curves. The solid line represents an ROC curve with an AUC of 0.79392. The dashed line represents the ROC for a completely random classifier.

4.1.5 Genetic Programming

The purpose of the genetic programming step is to find the best composite feature for separating two classes by combining the individual features using a user-defined function set. The best composite feature created by the GP will depend on the fitness function used. Three fitness functions, two based on maximizing the Fisher discriminant ratio and one that evaluates each individual with a k-NN classifier, will be employed to develop composite features for each subject.

4.1.6 Classification

A k-NN classifier will be utilized to classify all voxels in the regions of interest. The composite feature value will be calculated for each voxel and will determine whether a given voxel is labeled as normal or epileptogenic. Leave-one-out validation will be used to evaluate the accuracy of each feature and determine which is best. Values of k = 3, 5, and 7 will be tested for the best accuracy. Support vector machines and fuzzy classifiers will be explored as well to account for uncertainty due to overlap in the feature space.

4.1.7 Phantom Data Generation

A phantom dataset will be created to validate the experimental results. The hemodynamic response of perfusion fMRI, which is similar to the BOLD response, will be modeled as a sum of two gamma functions [35, 36]. This model hemodynamic response function (HRF) will then be added to selected voxels of the resting perfusion data of a healthy control to simulate spontaneous epileptic activity in a patient. Since the exact location of the abnormal activity will be known, the efficacy of the proposed system can be demonstrated. This step will verify that the system does indeed classify the voxels based on the presence of epileptiform discharges, not merely noise or other random effects.

4.2 Work Completed

- Development of a voxel-based fMRI time series analysis routine that enables discrimination between normal brain and epileptic cortex
- Implementation of PCA and ICA based noise removal techniques
- Extraction and selection of features from BOLD fMRI time series data and classification of voxels as epileptogenic or normal
- Preliminary feature analysis of five ASL perfusion fMRI datasets (three epilepsy patients and two controls)

4.3 Work Remaining

- Analyze additional patient data as they become available
- Apply noise removal techniques to improve signal-to-noise ratio of ASL perfusion data
- Investigate additional features to better discriminate between normal and epileptogenic tissue and rank them using ROC analysis
- Analyze the data using patient specific masks
- Model the hemodynamic response and generate a phantom fMRI dataset to validate the feature selection and classification system
- Apply the fMRI analysis methodology to intracranial EEG and compare with perfusion fMRI localization

4.4 Expected Contributions

- A novel voxel-based methodology for mapping human epileptic networks through the analysis of ASL perfusion fMRI time series data

- A set of quantitative features from multiple domains for classifying neural activity as normal or epileptiform in temporal lobe epilepsy patients
- A system for generating patient specific composite features for discrimination between epileptic and normal brain voxels in ASL perfusion images
- A better understanding of the temporal dynamics of cerebral blood flow in epilepsy patients versus healthy controls

4.5 Facilities Needed

The computing facilities available for conducting the proposed research include a PC in the Intelligent Control Systems Laboratory with a 3GHz Intel Pentium 4 processor, 1 GB of RAM, and a 230 GB hard drive and a laptop with a 2 GHz Pentium M processor, 1 GB of RAM, and a 70 GB hard drive. Both machines are running Windows XP Professional and Matlab 7.0. These resources are sufficient for the proposed research.

The BOLD and ASL perfusion fMRI data analyzed in the preliminary research came from our laboratory's collaborators in the Center for Functional Neuroimaging at the University of Pennsylvania. As the subjects and scanning time become available, they will collect additional ASL perfusion data from epilepsy patients and normal controls. Intracranial EEG recordings may also be collected if the patients are implanted prior to surgery.

REFERENCES

[1] J. F. Wilson, "Searching for Epilepsy Solutions," *Ann Intern Med*, vol. 141, pp. 329-332, 2004.

[2] C. W. Bazil, "Comprehensive Care of the Epilepsy Patient -- Control, Comorbidity, and Cost," *Epilepsia*, vol. 45, pp. 3-12, 2004.

[3] V. L. Morgan, R. R. Price, A. Arain, P. Modur, and B. Abou-Khalil, "Resting functional MRI with temporal clustering analysis for localization of epileptic activity without EEG," *NeuroImage*, vol. 21, pp. 473-481, 2004.

[4] J. S. Khoury, R. S. Winokur, J. I. Tracy, and M. R. Sperling, "Predicting seizure frequency after epilepsy surgery," *Epilepsy Research*, vol. 67, pp. 89-99, 2005.

[5] J. A. Detre and T. F. Floyd, "Functional MRI and Its Applications to the Clinical Neurosciences," *Neuroscientist*, vol. 7, pp. 64-79, 2001.

[6] J. A. Detre and J. Wang, "Technical aspects and utility of fMRI using BOLD and ASL," *Clinical Neurophysiology*, vol. 113, pp. 621-634, 2002.

[7] P. Gloor, "Neuronal generators and the problem of localization in electroencephalography: application of volume conductor theory to electroencephalography," *Journal of Clinical Neurophysiology*, vol. 2, pp. 327-54, 1985.

[8] B. Litt, R. Esteller, J. Echauz, M. D'Alessandro, R. Shor, T. Henry, P. Pennell, C. Epstein, R. Bakay, M. Dichter, and G. Vachtsevanos, "Epileptic Seizures May Begin Hours in Advance of Clinical Onset: A Report of Five Patients," *Neuron*, vol. 30, pp. 51-64, 2001.

[9] J. E. Desmond, J. M. Sum, A. D. Wagner, J. B. Demb, P. K. Shear, G. H. Glover, J. D. E. Gabrieli, and M. J. Morrell, "Functional MRI measurement of language Lateralization in Wada-tested patients," *Brain*, vol. 118, pp. 1411-1419, 1995.

[10] J. R. Binder, S. J. Swanson, T. A. Hammeke, G. L. Morris, W. M. Mueller, M. Fischer, S. Benbadis, J. A. Frost, S. M. Rao, and V. M. Haughton, "Determination of language dominance using functional MRI: a comparison with the Wada test," *Neurology*, vol. 46, pp. 978-984, 1996.

[11] J. A. Detre, L. Maccotta, D. King, D. C. Alsop, G. Glosser, M. D'Esposito, E. Zarahn, G. K. Aguirre, and J. A. French, "Functional MRI lateralization of memory in temporal lobe epilepsy," *Neurology*, vol. 50, pp. 926-932, 1998.

[12] J. A. Detre, J. I. Sirven, D. C. Alsop, M. J. O'Connor, and J. A. French, "Localization of subclinical ictal activity by functional magnetic resonance imaging: Correlation with invasive monitoring," *Annals of Neurology*, vol. 38, pp. 618-624, 1995.

[13] R. L. Wolf, D. C. Alsop, I. Levy-Reis, P. T. Meyer, J. A. Maldjian, J. Gonzalez-Atavales, J. A. French, A. Alavi, and J. A. Detre, "Detection of Mesial Temporal Lobe Hypoperfusion in Patients with Temporal Lobe Epilepsy by Use of Arterial Spin Labeled Perfusion MR Imaging," *AJNR Am J Neuroradiol*, vol. 22, pp. 1334-1341, 2001.

[14] A. Salek-Haddadi, K. J. Friston, L. Lemieux, and D. R. Fish, "Studying spontaneous EEG activity with fMRI," *Brain Research Reviews*, vol. 43, pp. 110, 2003.

[15] L. Jäger, K. J. Werhahn, A. Hoffmann, S. Berthold, V. Scholz, J. Weber, S. Noachtar, and M. Reiser, "Focal Epileptiform Activity in the Brain: Detection with Spike-related Functional MR Imaging—Preliminary Results," *Radiology*, vol. 223, pp. 860-869, 2002.

[16] C.-G. Bénar, Y. Aghakhani, Y. Wang, A. Izenberg, A. Al-Asmi, F. Dubeau, and J. Gotman, "Quality of EEG in simultaneous EEG-fMRI for epilepsy," *Clinical Neurophysiology*, vol. 114, pp. 569, 2003.

[17] A. Hoffmann, L. Jäger, K. J. Werhahn, M. Jaschke, S. Noachtar, and M. Reiser, "Electroencephalography during functional echo-planar imaging: Detection of epileptic spikes using post-processing methods," *Magnetic Resonance in Medicine*, vol. 44, pp. 791-798, 2000.

[18] J. Baudewig, H. J. Bittermann, W. Paulus, and J. Frahm, "Simultaneous EEG and functional MRI of epileptic activity: a case report," *Clinical Neurophysiology*, vol. 112, pp. 1196, 2001.

[19] W. Banzhaf, P. Nordin, R. E. Keller, and F. D. Francone, *Genetic Programming: An Introduction: On the Automatic Evolution of Computer Programs and Its Applications*. San Francisco, CA: Morgan Kaufmann Publishers, Inc., 1998.

[20] J. R. Koza, *Genetic Programming: On Programming of Computers by Means of Natural Selection*. Cambridge, MA: MIT Press, 1992.

[21] M. L. Rabin, V. M. Narayan, D. Y. Kimberg, D. J. Casasanto, G. Glosser, J. I. Tracy, J. A. French, M. R. Sperling, and J. A. Detre, "Functional MRI predicts post-surgical memory following temporal lobectomy," *Brain*, vol. 127, pp. 2286-2298, 2004.

[22] R. S. J. Frackowiak, K. J. Friston, C. Frith, R. Dolan, C. J. Price, S. Zeki, J. Ashburner, and W. D. Penny, *Human Brain Function*, 2nd ed: Academic Press, 2003.

[23] J. Wang, Z. Wang, G. K. Aguirre, and J. A. Detre, "To smooth or not to smooth? ROC analysis of perfusion fMRI data," *Magnetic Resonance Imaging*, vol. 23, pp. 75-81, 2005.

[24] K. J. Friston, J. Ashburner, C. D. Frith, J. B. Poline, J. D. Heather, and R. S. J. Frackowiak, "Spatial registration and normalization of images," *Human Brain Mapping*, vol. 3, pp. 165-189, 1995.

[25] K. J. Friston, A. P. Holmes, K. J. Worsley, J. P. Poline, C. D. Frith, and R. S. J. Frackowiak, "Statistical parametric maps in functional imaging: A general linear approach," *Human Brain Mapping*, vol. 2, pp. 189-210, 1994.

[26] J. A. Maldjian, P. J. Laurienti, and J. H. Burdette, "Precentral gyrus discrepancy in electronic versions of the Talairach atlas," *NeuroImage*, vol. 21, pp. 450-455, 2004.

[27] J. A. Maldjian, P. J. Laurienti, R. A. Kraft, and J. H. Burdette, "An automated method for neuroanatomic and cytoarchitectonic atlas-based interrogation of fMRI data sets," *NeuroImage*, vol. 19, pp. 1233-1239, 2003.

[28] N. Tzourio-Mazoyer, B. Landeau, D. Papathanassiou, F. Crivello, O. Etard, N. Delcroix, B. Mazoyer, and M. Joliot, "Automated Anatomical Labeling of Activations in SPM Using a Macroscopic Anatomical Parcellation of the MNI MRI Single-Subject Brain," *NeuroImage*, vol. 15, pp. 273-289, 2002.

[29] M. D'Alessandro, R. Esteller, G. Vachtsevanos, A. Hinson, J. Echauz, and B. Litt, "Epileptic seizure prediction using hybrid feature selection over multiple intracranial EEG electrode contacts: a report of four patients," *Biomedical Engineering, IEEE Transactions on*, vol. 50, pp. 603-615, 2003.

[30] J. Tanabe, D. Miller, J. Tregellas, R. Freedman, and F. G. Meyer, "Comparison of Detrending Methods for Optimal fMRI Preprocessing," *NeuroImage*, vol. 15, pp. 902, 2002.

[31] C. G. Thomas, R. A. Harshman, and R. S. Menon, "Noise Reduction in BOLD-Based fMRI Using Component Analysis," *NeuroImage*, vol. 17, pp. 1521, 2002.

[32] G. K. Aguirre, J. A. Detre, E. Zarahn, and D. C. Alsop, "Experimental Design and the Relative Sensitivity of BOLD and Perfusion fMRI," *NeuroImage*, vol. 15, pp. 488-500, 2002.

[33] J. Wang, Y. Zhang, R. L. Wolf, A. C. Roc, D. C. Alsop, and J. A. Detre, "Amplitude-modulated Continuous Arterial Spin-labeling 3.0-T Perfusion MR Imaging with a Single Coil: Feasibility Study," *Radiology*, vol. 235, pp. 218-228, 2005.

[34] C. E. Metz, "Basic principles of ROC analysis," *Seminars In Nuclear Medicine*, vol. 8, pp. 283-98, 1978.

[35] D. A. Handwerker, J. M. Ollinger, and M. D'Esposito, "Variation of BOLD hemodynamic responses across subjects and brain regions and their effects on statistical analyses," *NeuroImage*, vol. 21, pp. 1639-1651, 2004.

[36] H.-L. Liu, Y. Pu, L. D. Nickerson, Y. Liu, P. T. Fox, and J.-H. Gao, "Comparison of the temporal response in perfusion and BOLD-based event-related functional MRI," *Magnetic Resonance in Medicine*, vol. 43, pp. 768-772, 2000.

APPENDIX A: GLOSSARY

cerebral cortex: the outermost layer of the cerebrum

contralateral: occurring on, affecting, or acting in conjunction with a part on the opposite side of the body

focus: a localized area of epilepsy or the chief site of a generalized disease or infection

hemodynamic: relating to the mechanics of blood circulation

ictal: of, relating to, or caused by a sudden attack or seizure

interictal: occurring between seizures

ipsilateral: situated or appearing on or affecting the same side of the body

perfusion: the pumping of a fluid through an organ or tissue

slice: two-dimensional cross-section of a three-dimensional medical image

subclinical seizure: a seizure detected by EEG, which has no clinical correlate

voxel: the smallest distinguishable part of a three-dimensional image